

TIME-DEPENDENT SIMULATION OF FREE-ELECTRON LASER AMPLIFIERS AND OSCILLATORS*

H.P. Freund[#], Science Applications International Corp., McLean, VA 22102 USA

Abstract

Time-dependent FEL simulations use a variety of techniques. Particle-in-cell codes have been used to simulate free-electron masers; however, this is not feasible at short wavelengths. Most simulations use a slowly varying envelope approximation in both in z and t , where the particles and fields are advanced in z using the same process as in steady-state simulations and then the time derivative describing slippage is applied. We describe the inclusion of this technique in the non-wiggler-averaged code MEDUSA, which is then applied to study temporal behavior amplifiers and oscillators.

INTRODUCTION

Time-dependent FEL simulations use a variety of techniques. Particle-in-cell codes have been used to simulate free-electron masers [1,2]; however, this is not feasible at short wavelengths. Most simulations use a slowly varying envelope approximation (SVEA). One such technique assumes that the envelope varies only in z combined with a field representation as an ensemble of discrete harmonics. This has been shown to be equivalent to a time-dependent simulation [3]; however, it is often computationally prohibitive. A second technique uses an SVEA in both in z and t [4], and the particles and fields are advanced in z using the same process as in steady-state simulations and then the time derivative describing slippage is applied. This is used in wiggler-averaged codes such as PERSEO [5] in 1-D and GINGER [6] and GENESIS [7] in 3-D. We describe the inclusion of this technique in the non-wiggler-averaged code MEDUSA [8], which is then applied to amplifiers and oscillators.

THE FORMULATION

The formulation follows closely on that for the steady-state formulation [8]. The electromagnetic field is represented as a superposition of Gauss-Hermite modes

$$\delta\mathbf{A}(\mathbf{x},t) = \hat{\mathbf{e}}_x \sum_{l,n,h} e_{l,n,h}(x,y) \left[\delta A_{l,n,h}^{(1)} \cos \varphi_h + \delta A_{l,n,h}^{(2)} \sin \varphi_h \right], \quad (1)$$

where “ l ” and “ n ” are transverse mode numbers, “ h ” is the harmonic number, $e_{l,n,h} = \exp(-r^2/w_h^2) H_l(\sqrt{2}x/w_h) H_n(\sqrt{2}y/w_h)$, H_l is the Hermite polynomial of order l , and w_h is the spot size, $\varphi_h = h(k_0 z - \omega t) + \alpha_h r^2/w_h^2$ ($k_0 = \omega/c$). We assume that $\delta A_{l,n,h}^{(1,2)}$, w_h , and α_h , vary slowly in z and t . The dynamical equations are

$$\left(\frac{d}{dz} + \frac{w_h'}{w_h} \right) \begin{pmatrix} \delta A_{l,n,h}^{(1)} \\ \delta A_{l,n,h}^{(2)} \end{pmatrix} + K_{l,n,h} \begin{pmatrix} \delta A_{l,n,h}^{(2)} \\ -\delta A_{l,n,h}^{(1)} \end{pmatrix} = \begin{pmatrix} s_{l,n,h}^{(1)} \\ s_{l,n,h}^{(2)} \end{pmatrix}, \quad (2)$$

where $\delta A_{l,n,h}^{(1,2)} = e \delta A_{l,n,h}^{(1,2)}/m_e c^2$, $d/dz = \partial/\partial z + c^{-1} \partial/\partial t$, the

“prime” superscript denotes the total z -derivative,

$$K_{l,n,h} = (l+n+1) \left(\alpha_h \frac{w_h'}{w_h} - \frac{\alpha_h'}{2} - \frac{1+\alpha_h^2}{hk_0 w_h^2} \right), \quad (3)$$

$$\begin{pmatrix} s_{l,n,h}^{(1)} \\ s_{l,n,h}^{(2)} \end{pmatrix} = \frac{2\omega_b^2}{h\omega_0 c} \frac{F_{l,n}}{w_h^2} \left\langle \frac{v_x}{|v_z|} e_{l,n,h} \begin{pmatrix} \cos \varphi_h \\ -\sin \varphi_h \end{pmatrix} \right\rangle, \quad (4)$$

where $\omega_b(z,t)^2 = 4\pi e^2 n_b(z,t)/m_e$ for a beam density n_b , and $F_{l,n} = [2^{l+n} l! n!]^{-1}$. Note that the beam density varies to account for the temporal profile of the pulse. For a beam with a Gaussian energy and phase space distributions, the source terms are

$$\langle (\cdot) \rangle \equiv \int_0^{2\pi} \frac{d\psi_0}{2\pi} \int_0^\infty d\gamma_0 \frac{\exp[-(\gamma - \bar{\gamma}_0)^2/2\Delta\gamma^2]}{\sqrt{\pi/2} \Delta\gamma [1 + \operatorname{erf}(\bar{\gamma}_0/\sqrt{2}\Delta\gamma)]} \times \iiint dx_0 dy_0 dp_{x0} dp_{y0} \frac{\exp(-r_0^2/2\sigma_r^2 - p_{\perp 0}^2/2\sigma_p^2)}{(2\pi)^2 \sigma_r^2 \sigma_p^2} (\cdot), \quad (5)$$

and we assume, for simplicity, that only the current varies over the course of the pulse. The spot size and radius of curvature for each harmonic component are given by

$$w_h' = \frac{2\alpha_h}{hk_0 w_h} - w_h Y_h, \quad (6)$$

$$\frac{\alpha_h'}{2} = \frac{1+\alpha_h^2}{hk_0 w_h^2} - (X_h + \alpha_h Y_h), \quad (7)$$

and

$$X_h = 2 \frac{(s_{2,0,h}^{(1)} + s_{0,2,h}^{(1)}) \delta a_{0,0,h}^{(2)} - (s_{2,0,h}^{(2)} + s_{0,2,h}^{(2)}) \delta a_{0,0,h}^{(1)}}{\delta a_{0,0,h}^2}, \quad (8)$$

$$Y_h = -2 \frac{(s_{2,0,h}^{(1)} + s_{0,2,h}^{(1)}) \delta a_{0,0,h}^{(1)} + (s_{2,0,h}^{(2)} + s_{0,2,h}^{(2)}) \delta a_{0,0,h}^{(2)}}{\delta a_{0,0,h}^2}, \quad (9)$$

and $\delta a_{0,0,h}^2 = \delta a_{0,0,h}^{(1)2} + \delta a_{0,0,h}^{(2)2}$. These equations constitute the source-dependent expansion [9], which is a self-consistent adaptive eigenmode representation that tracks the optical guiding of the mode based upon the interaction with the electron beam

These field equations are integrated simultaneously with the complete Lorentz force equations for an ensemble of electrons. Here, we assume that the electron pulse shape is parabolic and we divide the pulse into slices corresponding to a beamlet one wavelength in length. The radiation field is also represented as a superposition of slices that correspond to the slices of the electron bunch. The *initial* condition for the radiation is chosen to represent a parabolic pulse shape as well.

*Work supported by the JTO, ONR, and NAVSEA.

[#]henry.p.freund@saic.com

Note that since MEDUSA uses a non-wiggler-averaged formalism, the step size in z must be small enough to resolve the wiggler-motion, and that the slippage is applied on every step.

AMPLIFIER MODELING

In simulating amplifiers, the initial radiation pulse is chosen to correspond to the electron pulse for a given peak seed power. As the electrons and radiation propagate through the wiggler, the radiation slips ahead of the electrons (one wavelength per wiggler period at resonance); hence, the simulation must include additional slices of the radiation pulse ahead of the electrons but which start at zero power and have no corresponding electron slice.

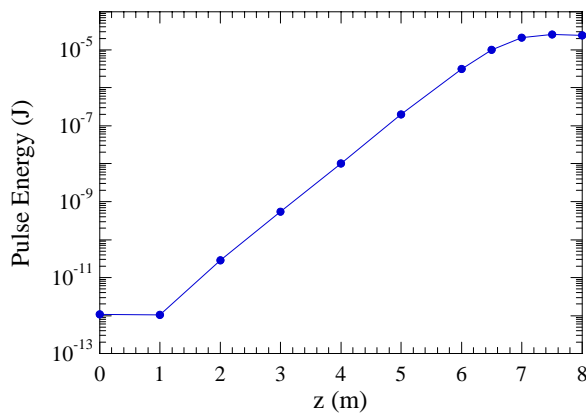


Figure 1: Growth of the pulse energy through the wiggler.

As an example showing slippage in amplifiers, we use a 76 MeV/400 A electron beam with an emittance of 15 mm-mrad, an energy spread of 0.1%, and a pulse time of 1 psec. The wiggler amplitude is 7.5 kG with a period of 2.18 cm, which yields a resonance at a wavelength of 1.06 microns. A seed power of 1 W is assumed. The growth of the pulse energy through the wiggler is shown in Fig. 1. Exponential growth is evident and saturation is found after about 7.5 m with a 25 μ J pulse energy corresponding to a peak power of 74 MW.

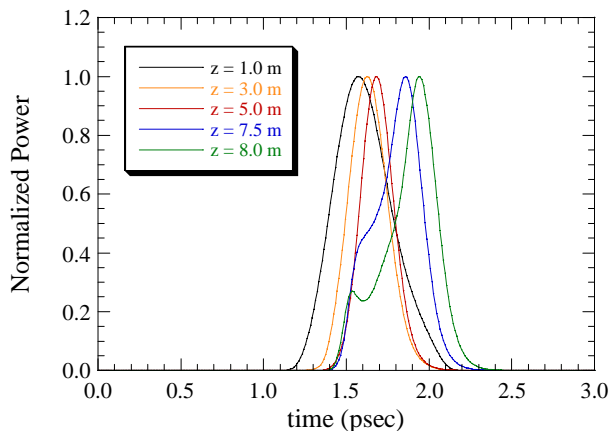


Figure 2: Evolution of radiation pulse shapes versus time.

Radiation slippage through the wiggler results in a pulse with both slips ahead of the electrons and distorts in shape from the original parabolic profile. This is illustrated in Fig. 2 where we plot the normalized power in the pulse at various points in the wiggler. The initial pulse is parabolic with a 1 psec duration, and the center of the electron bunch is at 1.5 psec in the figure. It is clear that as the interaction proceeds, the radiation slips significantly ahead of the electrons and is distorted in shape and narrowed in duration.

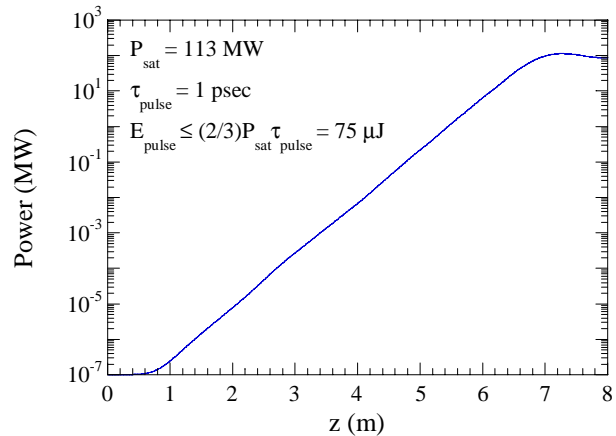


Figure 3: Power growth in a steady-state simulation.

Since the slippage time is comparable to the pulse duration, we expect that slippage will significantly reduce the power and pulse energy relative to that from a steady-state simulation. For comparison, we show the results of a steady-state simulation in Fig. 3 where we find a much higher peak power of 113 MW. If we assume that the pulse is parabolic and does not distort over the course of the interaction, then the pulse energy is given by $E_{pulse} = (2/3)P_{sat}\tau_{pulse}$. This implies that the pulse energy at saturation would be about 75 μ J. This dramatically illustrates the reductions in performance due to slippage when the slippage time is comparable to the pulse duration.

OSCILLATOR MODELING

The procedure for modeling oscillators in MEDUSA is illustrated schematically in Fig. 4. The wiggler is located in the center of the resonator. The electron beam is injected into the wiggler/resonator and amplifies what is initially (*i.e.*, at the entrance to the wiggler) an ensemble of vacuum resonator modes $[\{TEM\}_{l,n}]$. The mode is both amplified and guided in the wiggler; hence, it is focused to a smaller spot at the wiggler exit than would be found in the vacuum resonator. This “dressed” ensemble of resonator modes $[\{TEM\}_{l,n}]$ is then decomposed into a new ensemble of vacuum resonator modes $[\{TEM\}_{l,n}^{(new)}]$, which is “propagated” back to the wiggler entrance where it interacts with another electron bunch.

This process is repeated an arbitrary number of times until the system reaches a steady state.

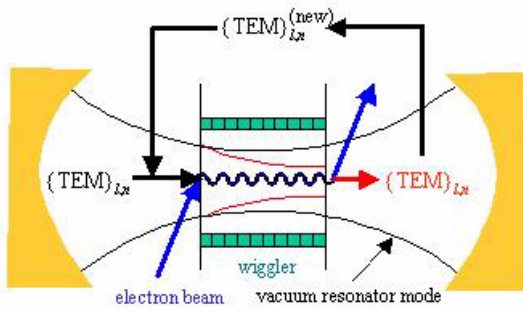


Figure 4: Schematic of oscillator feedback.

In simulating slippage in oscillators, the initial condition for the first pass around the resonator is the same as for the treatment of amplifiers, but subsequent passes must account for cavity detuning. Depending on the cavity length, the radiation pulse may arrive ahead or behind the electron bunch. Therefore, it is necessary to include “blank” radiation slices both ahead and behind the electron bunch and to shift the overlap of the radiation and electron slices on each pass based on the electron bunch repetition rate and the radiation round trip time in the resonator.

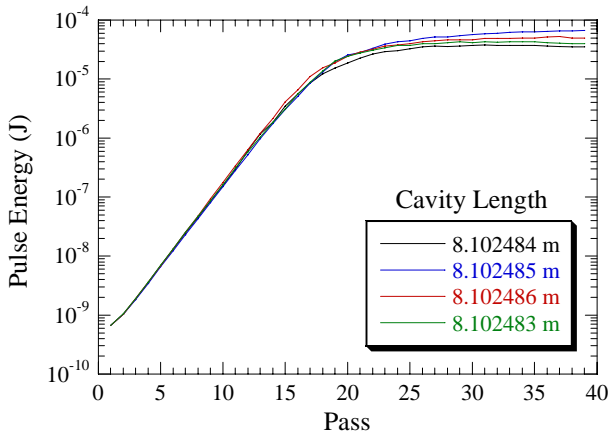


Figure 5: Growth of the pulse energy versus pass.

The example we consider employs a 47.15 MeV/60 A (peak current) electron beam with an emittance of 7 mm-rad in the wiggler plane and 8 mm-rad in the plane normal to the wiggler plane. For computational simplicity, we also assume that the energy spread vanishes. The pulse duration is assumed to be 1 psec and the pulse repetition rate is 37 MHz, which corresponds to a duty factor of 3.7×10^{-5} . We assume that the wiggler amplitude is 5.5 kG, the period is 2.7 cm, and the length is 41 periods. This yields a resonance at a wavelength of 3.11 microns. The waist size in the resonator is taken to be 628 microns, and we assume that 10% of the power is out-coupled. The optimal cavity tuning is dependent upon the transit time through the resonator and the repetition rate of the

electron bunches. The optimal cavity length is found to be 8.102485 m for which we find that the peak pulse energy in the resonator is 67 μ J. In view of the duty factor and resonator out-coupling, this yields an average output power of about 250 W. The evolution of the pulse energy versus pass is shown in Fig. 5 for a variety of different cavity lengths in the neighborhood of the optimum cavity length, and shows a fairly rapid decline in pulse energy as the cavity length shifts away from the optimum value.

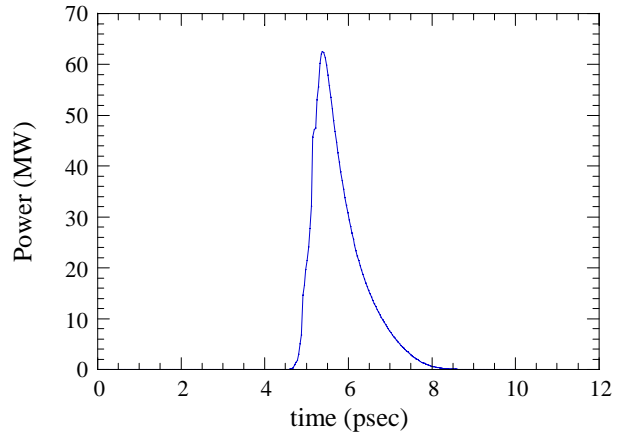


Figure 6: Pulse shape after 40 passes through the wiggler for a cavity length of 8.102485 m.

Accounting for this slippage as well as the cavity tuning, the distortion of the radiation pulse corresponding to the optimal cavity length after 40 passes is given in Fig. 6, and shows a sharp trailing edge with a more gradual decline in the leading edge. We also observe that, due to the cavity tuning, the total pulse width has broadened although the FWHM width remains about 1 psec.

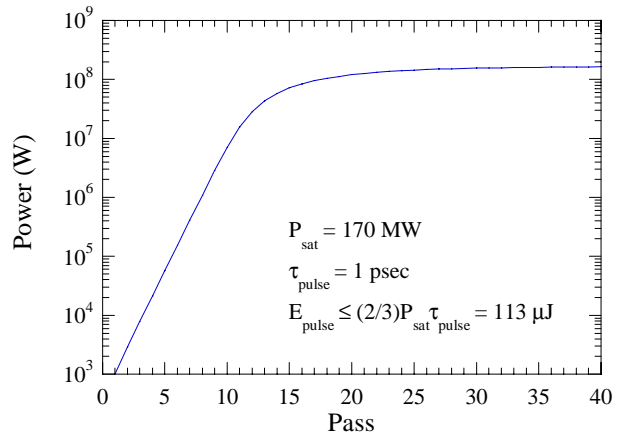


Figure 7: Steady-state oscillator simulation.

The slippage time through the wiggler for this example is about 0.4 psec. This is comparable to pulse duration, and we would expect that slippage has a negative effect on the oscillator power. This is illustrated in a steady-state simulation shown in Fig. 7, where we note that in comparison, the steady-state simulation for these

oscillator parameters yields a peak power of 170 MW. Assuming a parabolic pulse shape that is undistorted by the interaction, we note that this corresponds to a peak pulse energy of about 113 μ J and an average output power of about 629 W.

SUMMARY

The associated effects of time-dependence and slippage have been incorporated into the non-wiggler-averaged MEDUSA simulation code, and the results applied to both amplifier and oscillator configurations. As expected, when the slippage time is comparable to the duration of the electron pulses, slippage is seen to have a significant negative impact on the FEL interaction.

REFERENCES

- [1] T.J.T. Kwan *et al.*, Phys. Fluids **20**, (1977) 581.
- [2] A.T. Lin *et al.*, Phys. Fluids **26**, (1983) 3.
- [3] N. Piovella, Phys. Plasmas **6**, (1999) 3358.
- [4] R. Bonifacio *et al.*, Phys. Rev. A **40**, (1989) 4467.
- [5] L. Giannessi, PERSEO reference available at www.perseo.enea.it.
- [6] W. Fawley, "An informal Manual for GINGER and its post-processor XPLOTGIN", LBID-2141, CBP Tech Note-104, UC-414, 1995.
- [7] S. Reiche, Nucl. Instrum. Meth. **A429**, (1999) 243.
- [8] H.P. Freund *et al.*, IEEE J. Quantum Electron. **36**, (2000) 275.
- [9] P.A. Sprangle *et al.*, Phys. Rev. A **36**, (1987) 202.